THEORETICAL STUDY OF SUBSTITUENT EFFECTS IN THE UNIMOLECULAR DECOMPOSITION OF N-CHLORO-α-AMINO ACID ANIONS. ANALYSIS OF TRANSITION STRUCTURE AND MOLECULAR REACTION MECHANISM

J. ANDRÉS,* J. J. QUERALT AND V. S. SAFONT

Department of Experimental Sciences, Universitat Jaume I Castelló, Apartat 242, E-12080 Castelló, Spain

AND

M. CANLE AND J. A. SANTABALLA

Departamento de Química Fundamental e Industrial, Facultad de Ciencias, Universidad de La Coruña, A Zapateira s/n, E-15071 La Coruña, Spain

The unimolecular decomposition of substituted N-chloro-α-glycine anions was examined by an *ab initio* method using the 6–31G* basis set to obtain an insight into the relationship between transition-state structure and reactivity. The complete potential energy surface was explored and the stationary points corresponding to reactant and transition structure were localized. A reaction analysis by correlation of bond orders revealed that the reaction mechanism corresponds to an asynchronous fragmentation. The transition structure for all the compounds has an antiperiplanar conformation between the C—C and N—Cl bond breaking and it has a product-like character. The influence of the substitution on the α-carbon and on the nitrogen is discussed. When the size and number of substituents on the α-carbon and to a lesser extent on the nitrogen atom increase the relative energy decreases. The size of the substituent produces perpendicular effects and the type and number of substituents give parallel effects.

INTRODUCTION

The prediction of reaction pathways in the gas phase using quantun mechanical calculations has contributed to a greater understanding of a wide range of chemical reactions.[1] Theoretical studies of reaction mechanisms provide a powerful tool in physical organic chemistry for characterizing transition structures (TS). Their location in the region of the potential energy surface (PES) holds the key to obtaining a fundamental understanding of reaction kinetic data.[2] The properties of TS are responsible for, and can be related to, the observed kinetic behaviour of organic reactions in solution.

N-Chloro-α-amino acids of well known environmental and synthetic interest[3–5] are formed readily in aqueous solution from the reaction of amino acids with chlorinating agents, but they are not stable systems and decompose to ammonia, chloride ion and carbonyl compounds possessing one less carbon atom (Strecker degradation),[6] via a three-step mechanism, the second step being rate limiting:[7]

$$R_2R_3C = NH \xrightarrow{H_2O} R_2R_3CO + NH_3 \quad (3)$$
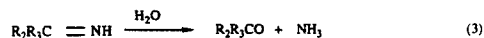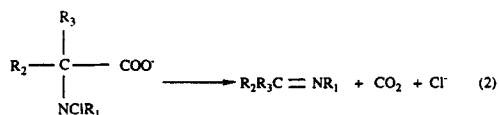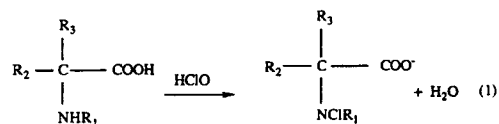
Several studies have been carried out in order to establish the nature of the molecular mechanisms for the decomposition of these systems.[7–16] Fox and Bullock[4] put forward a two-step mechanism: initial loss of the α-

---

* Author for correspondence.

proton followed by dechlorination of the intermediate carbanion. Grob and Schiess suggested that these reactions can be classified as a fragmentation process, while Hand *et al.* proposed a concerted unimolecular fragmentation process.

In a recent study,[17] we obtained the TSs for the decomposition of the anionic form of *N*-chloro-α-glycine with semi-empirical and *ab initio* methods and have found that the fundamental features of the reaction path are well represented when the calculations are performed with 6–31G* basis set. All our theoretical results are consistent with a concerted fragmentation mechanism. In this study, we decided to deal with substituted anions of the *N*-chloro-α-glycine, which allow calculations to be performed at a fairly sophisticated level, but which also permit systematic variation of the molecule substitution. In this paper, we report results of an investigation of more complex model systems, describing structure–activity studies carried out on different *N*-chloro-α-amino acids which were designed to determine the nature of their molecular mechanism for decomposition process in more detail.

COMPUTATIONAL METHOD AND MODELS

All calculations were carried out using the Gaussian 92 package.[18] The *ab initio* gradient approach is an efficient tool for the theoretical investigation of the PES, although its results may be impaired by errors from the correlation energy. *Ab initio* calculations were performed at HF/6–31G* basis set level. A previous comparative analysis[17] between different computational methods has demonstrated that, for our systems, the use of diffuse functions with the 6–311+G* basis set does not yield sensitive changes either in the numerical results or in the main conclusions obtained. The selected 6–31G* basis set can be considered as an adequate compromise between accuracy and computing time. In fact, this basis set has been used by other workers[19–21] in recent studies involving anionic and zwitterionic species with good results. Clark *et al.*[22] demonstrated that the inclusion of diffuse functions in the basis set is necessary to describe anions where there is a localized negative charge.

The selected models are the anionic forms of the following *N*-chloro-α-amino acids, NClR$_1$—CR$_2$R$_3$—COO$^-$:   R$_1$ = R$_2$ = R$_3$ = H,   *N*-chloroglycine   (I); R$_1$ = R$_2$ = H   R$_3$ = CH$_3$,   *N*-chloroalanine   (II); R$_1$ = R$_2$ = H,   R$_3$ = CH$_2$CH$_3$,   *N*-chloro-2-aminobutyric acid (III); R$_1$ = R$_2$ = H, R$_3$ = CH$_2$OH, *N*-chloroserine (IV); R$_1$ = CH$_3$, R$_2$ = R$_3$ = H, *N*-chlrosarcosine (V); R$_1$ = CH$_2$CH$_3$ R$_2$ = R$_3$ = H,   *N*-chloro-*N*-ethylglycine (VI); R$_1$ = H, R$_2$ = R$_3$ = CH$_3$, *N*-chloro-*N*-aminoisobutyric acid (VII); R$_1$ = R$_3$ = CH$_3$, R$_2$ = H, *N*-chloro-*N*-methylalanine   (VIII);   R$_2$ = H,   R$_1$ + R$_3$ = —CH$_2$CH$_2$CH$_2$—,   *N*-chloroproline   (IX); R$_1$ = R$_2$ = R$_3$ = CH$_3$,   *N*-chloro-*N*-methyl-2-aminoisobu-

tyric acid (X). The atom numbering for the selected models is depicted in Figure 1.

Geometries were optimized with the help of the Berny analytical gradient optimization routines.[23,24] The required convergence on the density matrix was 10^{-9} atomic units, and the threshold value of maximum displacement was 0·0018 Å and that of maximum force was 0·00045 hartree bohr^{-1}. TS searching was performed within all calculation levels with an 'eigenvalue following' optimization method.[25,26] The nature of a particular stationary point on the PES was confirmed by the number of imaginary frequencies. All TSs possess only one imaginary frequency, whereas all minima have none.

The transition vectors and force constants allow us to decide which variables control the transformation. The evolution of electron distribution helps us to interpret the results. Changes of bond orders explain the nature of the process.
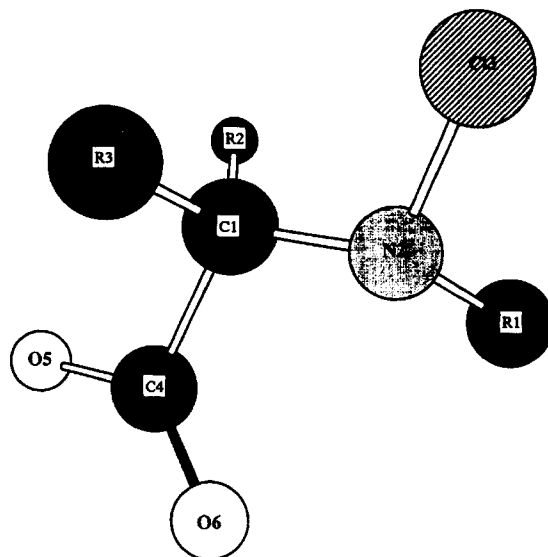
R$_1$=R$_2$=R$_3$=H, N-Chloroglycine (I)

R$_1$=R$_2$=H; R$_3$=-CH$_3$, N-Chloroalanine (II)

R$_1$=R$_2$=H; R$_3$=-CH$_2$CH$_3$, N-Chloro-2-amino-butyric acid (III)

R$_1$=R$_2$=H; R$_3$=-CH$_2$OH, N-Chloroserine (IV)

R$_1$=-CH$_3$; R$_2$=R$_3$=H, N-Chlorosarcosine (V)

R$_1$=-CH$_2$CH$_3$; R$_2$=R$_3$=H, N-Chloro-N-ethylglycine (VI)

R$_1$=H; R$_2$=R$_3$=-CH$_3$, N-Chloro-2-amino-isobutyric acid (VII)

R$_1$=R$_3$=-CH$_3$; R$_2$=H, N-Chloro-N-methylalanine (VIII)

R$_1$+R$_3$=-CH$_2$-CH$_2$-CH$_2$-; R$_2$=H, N-Chloroproline (IX)

R$_1$=R$_2$=R$_3$=-CH$_3$, N-Chloro-N-methyl-2-amino-isobutyric acid (X)

Figure 1. Numbering of the atoms for the anionic forms of the different *N*-chloro-α-amino acids employed

RESULTS AND DISCUSSION

3.1 Energetics of stationary points

In Table 1, total and relative (ΔE) energies between reactants (R) and TS, activation enthalpy ($\Delta H\ddagger$) and activation entropy ($\Delta S\ddagger$) for anionic forms of different *N*-chloro-α-amino acids are reported. Relative energies vary between 11 and 43 kcal mol^{-1} (1 kcal = 4·184 kJ). There are five distinct sets of values: IX, 11 kcal mol^{-1}; III, VII and X, 14–15 kcal mol^{-1}; I, VI and VIII, 18–19 kcal mol^{-1}; V, 22 kcal mol^{-1}; and II and IV, 42–43 kcal mol^{-1}. The experimental values reported in the literature range between 19 and 34 kcal mol.[27,28] All systems present positive and low values for the activation entropy. These positive values are in accordance with the expected entropic behaviour for a unimolecular fragmentation.

Links can be established between energetics and different substituents. There is a relationship between the size of the substituent on C-1 and the energetic barrier: the change of the methyl group for an ethyl group, II and III, decreases the barrier height from 43 to 14 kcal mol,$^{-1}$ whereas the change of the methyl group for a methoxy group, II to IV renders a similar value. This effect is less pronounced for the substitution on the N centre; the difference in ΔE between V and VI is only 3 kcal mol^{-1}. There is another relationship with respect to the number of substituents: when the *N*-chloro-α-amino acid is disubstituted at C-1 or N atoms, changing from II to VII or II to VIII the barrier height decreases by 28 and 24 kcal mol^{-1}, respectively. These facts agree with the experimental results.[8,9] A comparison of ΔE values among VII (methyl disubstitution on C-1 α-carbon atom), VIII (methyl disubstitution on C-1 and N atoms), IX (proline) and X (methyl trisubstitution on C-1 and N atoms) indicates that N substitutions are of less importance than C-1 α-carbon substitutions. It is important to note that I shows anomalous behavior; this has been previously noted from experimental results.[27]

3.2. Structures of stationary points

The geometrical parameters for R and TS obtained with the different *N*-chloro-α-amino acids are presented in Tables 2 and 3, respectively. It is important to note that the geometrical parameters corresponding to R and TS are similar, except for the dihedral angle τ(Cl-3—N-2-C-1—C-4). It is a measure of the antiplanarity between the Cl-3 and C-4 centres. The values range from 147 to 179° and 137 to 179° for R and TS, respectively. This conformation provides a large overlap of π-orbitals to yield the C-1—N-2 double bond and it permits the readily formation of the TS and the development of unimolecular fragmentation. These results show that the variation in ΔE does not necessarily reflect the real variation in the TS. In other words, it is not always correct to draw a conclusion on the variation in the TS from the variation of the barrier height.

Another possibility for comparing the similarity of TSs is to determine the transition vector (TV).[29] The unique negative eigenvalue from the diagonalization of the Hessian, the imaginary frequency, the force constants for those selected geometric parameters with non-zero components in the TV and corresponding components of the eigenvector in this control space are listed in Table 4. The TV for all TSs yields the essentials of the chemical process under study and the control space contains internal variables that define the chemical interconversion process. There are two dominant contributions in the TV, which are fairly invariant to the model system, as shown by a perusal of the amplitudes of the TV, i.e. the two bonds, C-1—C-4 and N-2—C-13, that are broken. The C-1—N-2 bond distance, which evolves from single to a double bond, has a minor participation in the TV. The TS is well associated in all cases with the decomposition process.

The magnitude of the eigenvalue, ranging from $-0·077$ to $-0·164$, which is related to the curvature of the potential energy surface, is remarkably constant.

Table 1. Total energy (a.u.) of reactants (R) and TSs obtained for the decomposition process of the anionic form of the different *N*-chloro-α-amino acids: relative energy for TS (ΔE) in kcal mol^{-1}, activation enthalpy ($\Delta H\ddagger$) in kcal mol^{-1} and activation entropy ($\Delta S\ddagger$) in cal mol^{-1} k^{-1}

Compound	Total energy of R	Total energy of TS	ΔE	$\Delta H\ddagger$	$\Delta S\ddagger$
I	−741·129174	−741·099844	18·40	15·77	2
II	−780·163141	−780·094389	43·14	39·55	3
III	−819·196589	−819·173822	14·19	11·68	2
IV	−855·022332	−854·955220	42·11	38·39	4
V	−780·150938	−780·116495	21·61	18·28	1
VI	−859·179155	−859·150322	18·09	14·90	0
VII	−819·200440	−819·176758	14·86	12·29	2
VIII	−819·182116	−819·151974	18·91	15·99	0
IX	−857·055599	−857·038054	11·01	8·76	1
X	−858·211225	−858·187747	14·73	11·89	0

Table 2. Relevant geometric parameters for reactants

Parameter[a]	I	II	III	IV	V	VI	VII	VIII	IX	X
r(C1—N2)	1·460	1·465	1·472	1·461	1·464	1·467	1·471	1·463	1·475	1·477
r(N2—Cl3)	1·762	1·762	1·765	1·747	1·780	1·778	1·763	1·771	1·795	1·776
r(C1—C4)	1·560	1·567	1·568	1·562	1·566	1·569	1·580	1·582	1·570	1·600
r(C4—O5)	1·236	1·236	1·237	1·247	1·229	1·226	1·225	1·229	1·229	1·230
r(C4—O6)	1·225	1·226	1·225	1·219	1·229	1·232	1·225	1·230	1·231	1·228
r(C1—R2)	1·082	1·082	1·083	1·083	1·090	1·088	1·526	1·090	1·078	1·532
r(C1—R3)	1·087	1·538	1·536	1·533	1·081	1·081	1·538	1·526	1·545	1·543
r(C1—R1)	1·004	1·003	1·000	1·000	1·451	1·455	1·003	1·445	1·465	1·449
∠(R2—C1—R3)	108·15	109·32	109·90	109·04	107·46	108·26	110·04	107·67	112·52	107·18
∠(C1—N2—Cl3)	112·58	115·48	115·64	115·86	108·66	108·43	115·65	110·37	110·02	111·16
∠(Cl3—N2—R1)	104·88	105·53	105·72	106·67	107·09	107·09	105·31	109·02	107·78	109·02
∠(C1—N2—R1)	105·34	106·45	102·00	107·72	114·32	114·43	106·25	116·24	103·89	115·80
∠(C1—C4—O5)	114·63	114·68	113·72	113·04	118·34	116·44	114·57	117·80	118·13	112·97
∠(O5—C4—O6)	130·76	130·59	130·47	130·10	130·48	130·74	130·14	130·08	130·38	129·56
τ(Cl3—N2—C1—C4)	-147·06	-157·79	162·01	-159·96	-174·39	-160·90	-154·01	179·16	-163·33	-174·55

[a] For numbering of atoms, see Figure 1. All distances (r) in Å and angles (∠) and dihedral angles (τ) in degrees.

Table 3. Relevant geometric parameters for TSs

Parameter[a]	I	II	III	IV	V	VI	VII	VIII	IX	X
r(C1—N2)	1·347	1·379	1·354	1·366	1·352	1·357	1·361	1·364	1·371	1·370
r(N2—Cl3)	2·249	2·320	2·227	2·362	2·348	2·393	2·220	2·274	2·275	2·265
r(C1—C4)	1·833	1·780	1·817	1·793	1·881	1·855	1·832	1·843	1·775	1·869
r(C4—O5)	1·200	1·200	1·196	1·191	1·191	1·195	1·196	1·193	1·207	1·191
r(C4—O6)	1·193	1·208	1·203	1·216	1·187	1·189	1·204	1·201	1·200	1·200
r(C1—R2)	1·076	1·076	1·078	1·078	1·076	1·076	1·542	1·077	1·074	1·528
r(C1—R3)	1·083	1·520	1·520	1·522	1·083	1·083	1·523	1·526	1·527	1·520
r(C1—R1)	1·002	1·015	1·000	1·014	1·443	1·444	1·015	1·445	1·459	1·448
∠(R2—C1—R3)	114·16	116·01	114·09	117·89	107·88	107·88	113·72	112·55	118·02	112·02
∠(C1—N2—Cl3)	111·23	107·96	112·23	106·95	105·71	100·94	112·22	116·94	110·00	116·94
∠(Cl3—N2—R1)	86·19	69·85	87·55	67·69	98·76	98·76	88·12	107·66	98·28	107·66
∠(C1—N2—R1)	109·64	106·04	109·93	111·00	116·83	118·26	109·81	113·81	106·32	114·42
∠(C1—C4—O5)	110·17	111·13	110·75	111·76	106·78	107·56	110·13	108·23	117·04	110·17
∠(O5—C4—O6)	140·82	137·95	139·48	137·68	142·97	141·80	139·08	139·71	137·62	139·57
τ(Cl3—N2—C1—C4)	159·24	137·58	166·16	136·99	-178·62	-178·78	-166·31	155·44	168·04	174·36

[a] See footnote to Table 2.

Table 4. Hessian unique negative eigenvalues (a.u.), imaginary frequencies (cm^{-1}) obtained from a normal mode analysis, force constants (F, a.u.) and Hessian eigenvector components (C) for the TSs

	I		II		III		IV		V		VI		VII		VIII		IX		X	
Eigenvalue	−0·11033		−0·08564		−0·11032		−0·08729		−0·07684		−0·07729		−0·10467		0·09002		−0·11777		−0·16406	
Imaginary frequency	610·80i		706·94i		589·75i		689·11i		594·48i		598·18i		576·68i		564·29i		497·86i		579·14i	
Parameter[a]	F	C	F	C	F	C	F	C	F	C	F	C	F	C	F	C	F	C	F	C
r(C1—N2)	0·48	−0·23	0·39	−0·24	0·47	−0·25	0·42	−0·24	0·45	−0·06	0·44	−0·19	0·47	−0·28	0·44	−0·23	0·49	−0·22	0·43	−0·21
r(N2—Cl3)	0·02	0·61	0·02	0·62	0·02	0·63	0·02	0·56	0·01	0·67	0·01	0·59	0·02	0·66	0·01	0·66	0·01	0·63	0·01	0·63
r(C1—C4)	0·05	0·64	0·09	0·53	0·06	0·60	0·09	0·54	0·04	0·71	0·04	0·73	0·07	0·56	0·06	0·61	0·08	0·63	0·07	0·61
∠(O5—C4—Cl)	0·56	−0·07	0·55	−0·09	0·59	−0·11	0·48	−0·10	0·50	−0·12	0·51	−0·18	0·55	−0·11	0·53	−0·15	0·61	−0·08	055	−0·15
∠(O6—C4—Cl)	0·50	−0·21	0·60	−0·16	0·52	−0·18	0·54	−0·15	0·49	−0·11	0·50	−0·15	0·60	−0·13	0·59	−0·13	0·32	−0·09	0·59	−0·10

[a] See footnote to Table 2.

The normal mode analysis of these structures yields a relatively low imaginary frequency, $500-700$ cm^{-1}, indicating that the quadratic zones around TS are flat and associated with the heavy atom motions. The force constants for C-1—C-4 and N-2—C-13 bond distances are very low, ranging from 0.01 to 0.09 and from 0.01 to 0.02 a.u., respectively, showing that these bonds are partially broken at the TS; however, the C-1—N-2 bond presents a larger value, $0.39-0.49$ a.u.

Bond orders

The variation of bond orders (*BO*) has been used to study the molecular mechanism of chemical reactions.[30-32] In order to follow the nature of the decomposition process, a two-dimensional diagram in terms of C-1—C-4 vs N-2—C-13 *BO* is used. The lower-left corner represents R and the upper-left and lower-right corners correspond to hypothetical intermediate structures. The reactions follow lines connecting the positions of the R and TS. The reaction path R–TS is described by the slopes α of these lines. A diagonal connection between R and TS represents a synchronous process, and the opposite corners represent a stepwise mechanism. The treatment of this diagram predicts that a given perturbation of the TS should produce a displacement parallel to the diagonal or perpendicular to it. The amount and direction of the movement depend on structural and electronic features which can change the energies of R and the corners. Therefore, the perpendicular and parallel effects to the reaction profile elaborated by Thornton[33] can be considered: substituent parallel effects to the reaction pathway, named 'Hammond effects', lead to a TS resembling more closely the opposite stabilized species, whereas substituent perpendicular effects, named 'anti-Hammond effects,' lead to a TS that has a greater likeness to the species which has been stabilized. Thus, the stabilization of a point X out of the reaction pathway, i.e. carbanion and nitrenium-like species, will lead to a new reaction pathway in which the TS has been shifted towards the point of stabilization. The sum of both effects predicts the displacement of the TSs on the diagram.

In order to analyse parallel and perpendicular effects, Pauling bond orders[34] (*BO*) were calculated for TSs

through the following expression:

$$BO = \exp\{[R(1) - R(TS)]/0.3\}$$

where $R(TS)$ represents the length corresponding to a bond in TS and $R(1)$ represents the reference bond length. For the breaking bonds (C-1—C-4 and N-2—Cl-3), the reference values considered were the equilibrium distances in reactants and for the C-1—N-2 bond, that evolves from single to double, the reference value was the equilibrium length of the double bond in the corresponding methylimine. Calculated percentages *BO* and α values for TSs are reported in Table 5. The percentage of C-1—C-4 and N-2—Cl-3 bonds breaking at the TS are in the range $50-65$ and $78-87$, respectively, while the C-1—N-2 bond change from single to double is in the range $65-73$. This description shows that the TS in an advanced stage of the reaction path, closer to products than to the reactants, having a product-like character. The transformation of the N-2—Cl-3 bond is more advanced than the C-1—N-2 and C-1—C-4 bonds. The molecular mechanism corresponds to an asynchronous fragmentation process. These facts are in accordance with experimental data.[27]

Comparisons between the different effects of substituents with respect to their size, type or number can be carried out. The different comparisons are depicted by solid arrows in Figure 2. Comparing II with III and V with VI, the substituent changes from methyl to ethyl on the C-1 α-carbon atom and on the nitrogen atom, respectively. Moving from II ($\alpha = 0.6$) to III ($\alpha = 0.69$), the percentage of C-1—C-4 bond breaking is larger and the percentage of N-2—Cl-3 bond breaking is smaller. An opposite effect is found for the change from V ($\alpha = 0.77$) to VI ($\alpha = 0.71$). Following the Thornton description, in the first case the TS will resemble more closely the carbanion-like species while in the second case the TS will be moved towards the hypothetical nitrenium-like intermediate. This can be explained by the fact that an increase in the size of the C-1 α-carbon substituent stabilizes the carbanion intermediate and an increase in the size of nitrogen substituent stabilizes the nitrenium-like intermediate.

With respect the type of substituent, on changing from II to IV, the methyl group is replaced by a methoxy group on the C-1 α-carbon atom. There is an

Table 5. Percentage of bond breaking at TSs for equilibrium length of C-1—C-4 and N-2—Cl-3 bonds and percentage of bond formation for equilibrium length of C-1—N-2 double bond

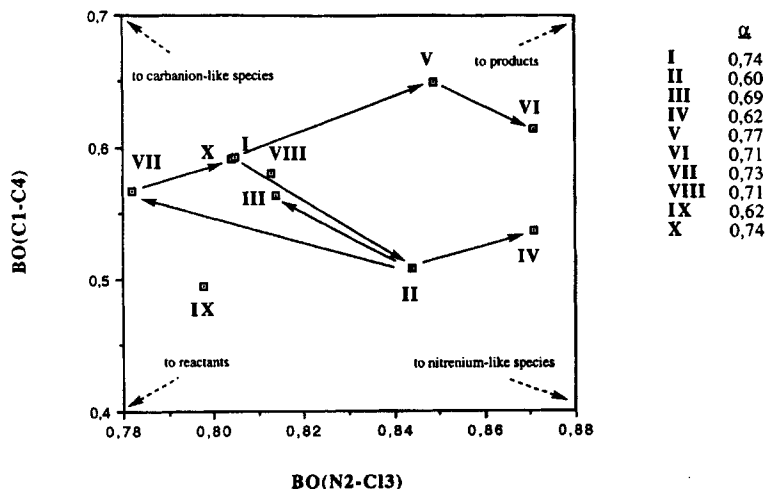| Bond	I	II	III	IV	V	VI	VII	VIII	IX	X
C-1—C-4	59·3	50·8	56·4	53·7	65·0	61·5	56·8	58·1	49·5	59·2
N-2—Cl-3	80·5	84·4	81·4	87·1	84·9	87·1	78·2	81·3	79·8	80·4
C-1—N-2	72·5	65·1	70·8	68·0	71·3	70·1	69·2	68·5	66·9	67·1

Figure 2. Two-dimensional diagram in terms of C-1—C-4 vs N-2—C-13 bond orders; α is the slope of the line that links R and TS. The different comparisons are depicted by solid arrows

increment in the percentages of breaking and making bonds. This implies a displacement towards the products due to the parallel effect; the perpendicular effects, measured by the α slopes, are similar: 0·60 and 0·62, respectively.

In order to gain an insight into the change in the number of the substituents, we first compare **II** and **VII** where the C-1 α-carbon becomes disubstituted with two methyl groups. The change from **II** to **VII** increases the percentage of C-1—C-4 bond breaking whereas it decreases the percentage of N-2—Cl-3 bond breaking. The slope α increases from 0·60 to 0·73. This increment displaces the TS closer to the carbanion-like species due to the presence of the second methyl group. If we now compare the effects of adding a methyl group on the N atom, two cases can be considered: from **I** to **V** and from **VII** to **X**. In both cases the percentages of the C-1—C-4 and N-2—Cl-3 breaking bonds are increased whereas the percentage of the C-1—N-2 forming bond decreases. There are only parallel effects: the TSs move towards P. The slope α has approximately the same values, 0·74–0·77 and 0·73–0·74, respectively. Moving from **I** to **X**, three hydrogens are substituted by three methyl groups, the TS location on the two-dimensional diagram is scarcely modified. Finally, we can compare **I** with **II**, where the C-1 α-carbon becomes monosubstituted by a methyl group. The slope α decreases from 0·74 to 0·60, i.e. the TS corresponding to **II** is more displaced towards the nitrenium-like species than TS for **I**. This change decreases the percentage of C-1—C-4 bond breaking whereas it increases the percentage of N-2—Cl-3 bond breaking. The perpendicular effect is larger than the parallel effect.

Population analysis

One step further in this analysis implies an understanding of the electronic changes undergone on going from R to TS. For this purpose, a Mulliken atomic population analysis is carried out. The choice of this kind of analysis over others, such as natural population analysis, is due to the fact that according to Otto and Ladik[35] and Mestres *et al.*,[36] they qualitatively yield the same trend of results. What is especially interesting is the analysis of the changes occurring until the TS has been reached. The results are presented in Table 6. There is a displacement of the negative atomic charge from the carboxylate (CO_2) to the chlorine (Cl-3) fragments, an increment of negative charge on the C-1 atom and an opposite effect on the N atom along the reaction path R–TS, in accordance with a unimolecular fragmentation process. The substitution of H by CH_3 or CH_2CH_3 in the C-1 α-carbon atom decreases its negative charge. A minor reduction is found when the substitution is carried out on the N atom.

Significant variations of charge distribution can be observed on the C-1 and N-2 centres for R and TS. First, it can be seen that the C-1 negative charge is always larger for TS than for R. On the other hand, the N-2 negative charge is always smaller for TS. This result reflects the fact that there is a larger charge separation in reactants than in TS: in R, the negative charge is accumulated at N-2, owing to its higher electronegativity. In TSs, this electronic density is displaced towards the bond between C-1 and N-2 because it is becoming a double bond.

For the net atomic charge on C-1 we can appreciate two well delimited cases: that in which the carbon has

Table 6. Net atomic charges for reactants and TSs calculated with the Mulliken population analysis

Atom	I R	I TS	II R	II TS	III R	III TS	IV R	IV TS	V R	V TS	VI R	VI TS	VII R	VII TS	VIII R	VIII TS	IX R	IX TS	X R	X TS
C-1	-0.23	-0.29	-0.06	-0.21	-0.07	-0.12	-0.09	-0.25	-0.23	-0.32	-0.22	-0.31	0.05	-0.01	-0.03	-0.15	-0.12	-0.12	0.07	-0.01
N-2	-0.68	-0.37	-0.69	-0.33	-0.68	-0.40	-0.70	-0.31	-0.51	-0.20	-0.52	-0.19	-0.69	-0.39	-0.54	-0.24	-0.49	-0.22	-0.53	-0.26
Cl-3	-0.07	-0.62	-0.06	-0.62	-0.06	-0.59	-0.02	-0.65	-0.07	-0.67	0.05	-0.70	-0.06	-0.58	-0.06	-0.67	-0.08	-0.61	-0.06	-0.62
C-4	0.75	0.76	0.76	0.78	0.77	0.77	0.75	0.79	0.75	0.77	0.74	0.77	0.79	0.79	0.74	0.79	0.77	0.78	078	0.81
O-5	-0.75	-0.63	-0.75	-0.63	-0.75	-0.64	-0.76	-0.60	-0.74	-0.60	-0.72	-0.61	-0.76	-0.63	-0.73	-0.61	-0.72	-0.65	-0.74	-0.61
O-6	-0.74	-0.61	-0.74	-0.66	-0.73	-0.63	-0.71	-0.69	-0.75	-0.59	-0.75	-0.59	-0.73	-0.65	-0.75	-0.63	-0.73	-0.64	-0.73	-0.63
CO_2	-0.74	-0.48	-0.73	-0.51	-0.71	-0.50	-0.72	-0.50	-0.74	-0.42	-0.73	-0.43	-0.70	-0.49	-0.74	-0.45	-0.75	-0.51	-0.69	-0.43
R_1	0.41	0.41	0.41	0.40	0.41	0.41	0.41	0.41	0.22	0.27	0.22	0.25	0.42	0.41	0.23	0.25	0.19	—	0.22	0.26
R_2	0.16	0.18	0.16	0.27	0.16	0.19	0.16	0.28	0.14	0.17	0.14	0.18	0.00	0.04	0.14	0.22	—	0.22	-0.02	0.00
R_3	0.15	0.18	-0.03	0.00	-0.04	0.03	-0.03	0.01	0.18	0.19	0.17	0.20	-0.01	0.01	-0.01	-0.01	—	—	-0.02	0.06

$^a CO_2 = C\text{-}4 + O\text{-}5 + O\text{-}6$.

no substituents, i.e., **I**, **V** and **VI**, the negative charge having major importance, in both R and TS; and the rest in which the negative charge is of minor importance. So it seems clear that the inclusion of the substituents considered here on the C-1 α-carbon produces a decrease in its negative charge. For the net atomic charge on N-2 the same effect can be observed.

CONCLUSIONS

The overall picture of the unimolecular decomposition of *N*-chloro-α-amino acid anions is complicated. The present theoretical calculations provide some new information which are complementary to the existing experimental data.

The reaction studied here involves two-bond breaking and one-bond making where the leaving groups are closed-shell species (chlorine anion and carbon dioxide) and, initially, one is not confronted with the usual shortcomings of the HF–SCF schemes.

The results of the present study can be summarized as follows:

(i) The reaction mechanism corresponds to a unimolecular asynchronous process.

(ii) At the TS, the C-1—C-4 and N-2—Cl-3 bond breaking and the C-1—N-2 double bond making are in advanced stages. In this sense, the TS is product-like and with an antiperiplanar conformation.

(iii) The TSs and TVs are independent of model systems. There is no correlation between the variations in barrier heights and TSs.

(iv) The increments in the size and number of substituents on the C-1 α-carbon and N atoms produce a decrease in ΔE. This effect is more pronounced on the C-1 centre.

(v) The size of the substituent produces opposite perpendicular effects depending on the substituted centre. The reaction path moves towards hypothetical carbanion or nitrenium-like species.

(vi) The type and number of substituents on C-1 and N render parallel effects.

(vii) The electronic reorganization along the reaction path R–TS corresponds to a unimolecular fragmentation process.

REFERENCES

1. V. I. Minkin, B. Ya Simkin and R. M. Minyaev, *Quantum Chemistry of Organic Compounds*, Ed. Springer-Verlag. Berlin-Heildelberg (1990).
2. I. H. Williams, *Chem. Soc. Rev.* 277 (1993).
3. J. Owusu-Yaw, W. B. Wheeler and C. I. Wei, *Water Chlorination (Environmental Science and Technology)*. Lewis, Midland, MI (1990).
4. S. M. Fox and M. W. Bullock, *J. Am. Chem. Soc.* **73**, 2754 (1951).
5. C. A. Grob and P. N. Schiess, *Angew. Chem. Int. Ed. Engl.* **6**, 1 (1967).
6. A. Schonberg and R. Moulbacher, *Chem. Rev.* **50**, 261 (1952).
7. W. D. Stambro and W. D. Smith, *Environ. Sci. Technol.* **13**, 446 (1979).
8. X. L. Armesto, L. M. Canle, M. Losada and J. A_ Santaballa, *J. Org. Chem.* **59**, 4659 (1994).
9. V. C. Hand, M. P. Snyder and D. W. Margeerum, *J. Am. Chem. Soc.* **105**, 4022 (1983).
10. R. Awad, A. Hussain and P. A. Crooks, *J. Chem. Soc., Perkin Trans. 2* 1233 (1990).
11. X. L. Armesto, L. M. Canle, M. Losada and J. Santaballa, *Int. J. Chem. Kinet.* **25**, 1 (1993).
12. X. L. Armesto, M. Canle, M. Losada and J. A. Santaballa, *Int. J. Chem. Kinet.* **25**, 331 (1993).
13. A. H. Friedman and S. Morgulis, *J. Am. Chem. Soc.* **58**, 909 (1936).
14. R. S. Ingols, H. A. Wyckoff, T. W. Kethley, H. W. Hasdgen, E. L. Fincher, J. C. Webrand and J. E. Mandl, *Ind. Eng. Chem.* **45**, 996 (1953).
15. J. M. Antelo, F. Arce, J. Franco, P. Rodriguez and A. Varela, *Int. J. Chem. Kinet.* **20**, 433 (1988).
16. J. M. Antelo, F. Arce, J. Crugeiras, J. Franco and J. A. Santaballa, *Int. J. Chem. Kinet.* **22**, 1271 (1990).
17. J. Andrés, J. J. Queralt, V. S. Safont, M. Canle and J. A. Santaballa, *J. Phys. Chem.* **100**, 3561 (1996).
18. M. J. Frisch, G. W. Trucks, M. Head-Gordon, P. M. W. Gill, M. W. Wong, J. B. Foresman, B. G. Johnson, H. B. Schlegel, M. A. Robb, E. S. Replogle, R. Gomperts, J. L. Andres, K. Raghavachari, J. S. Binkley, C. Gonzalez, R. L. Martin, D. J. Fox, D. J. Defrees, J. Baker, J. J. P. Stewart and J. A. Pople, *Gaussian92, Revision A*. Gaussian Pittsburg, PA (1992).
19. D. Yu, A. Rauk and D. A. Armstrong, *J. Am. Chem. Soc.* **117**, 1789 (1995).
20. J. H. Jensen and M. S. Gordon, *J. Am. Chem. Soc.* **117**, 8159 (1995).
21. R. Sustmann, W. Sicking and R. Huisgen, *J. Am. Chem. Soc.* **117**, 9679 (1995).
22. T. Clark, J. Chandrasekhar, G. W. Spitznagel and P. v. R. Schleyer, *J. Comput. Chem.* **4**, 294 (1983).
23. H. B. Schlegel, *J. Comput. Chem.* **3**, 214 (1982).
24. H. B. Schlegel, *J. Chem. Phys.* **77**, 3676 (1982).
25. J. Baker, *J. Comput. Chem.* **7**, 385 (1986).
26. J. Baker, *J. Comput. Chem.* **8**, 563 (1987).
27. M. Canle, Doctoral Thesis, Universidad de La Coruña (1994).

28. J. M. Antelo, F. Arce, J. Crugeiras, J. Franco, F. López, P. Rodríguez and A. Varela, *An. Quím.* **87**, 195 (1991).
29. R. W. Stanton and J. V. McIver, Jr. *J. Am. Chem. Soc.* **97**, 3632 (1975).
30. A. J. C. Varandas and S. J. F. Formosinho, *J. Chem. Soc., Faraday Trans. 2* 282 (1986).
31. G. Lendvay, *J. Mol. Struct. THEOCHEM* **167**, 331 (1988).

32. G. Lendvay, *J. Phys. Chem.* **93**, 4422 (1989).
33. E. R. Thornton, *J. Am. Chem. Soc.* **89**, 2915 (1967).
34. L. Pauling, *J. Am. Chem. Soc.* **69**, 542 (1947).
35. P. Otto and J. Ladik, *Int. J. Quantum Chem.* **18**, 1143 (1980).
36. J. Mestres, M. Duran and J. Bertrán, *Theor. Chim. Acta* **88**, 325 (1994).